MULTIPLE SCLEROSIS JOURNAL | MSJ

Original Research Paper

Clinical, structural, and functional MRI features predicting PIRMA at 5-year follow-up in multiple sclerosis

Multiple Sclerosis Journal

1–12

DOI: 10.1177/13524585261445318

Elena Barbuti, Claudia Piervincenzi, Viola Baione, Abhineet Ojha, Federica Satriano, Antonio Gallo, Alessandro D'Ambrosio, Nicola De Stefano, Rosa Cortese, Paola Valsasina, Carlo Pozzilli, Maria A Rocca, Massimo Filippi, and Patrizia Pantano; INNI Network*

Abstract

Objective: To identify baseline clinical, structural, and functional magnetic resonance imaging (MRI) features predicting progression independent of relapse and magnetic resonance imaging activity (PIRMA) in multiple sclerosis (MS).

Methods: We included patients from the Italian Neuroimaging Network Initiative who showed no clinical or MRI activity at 5-year follow-up. PIRMA progressors versus stable patients were defined by confirmed Expanded Disability Status Scale (EDSS) progression. Baseline clinical features, white matter (WM) lesion, WM, cortical and deep gray matter (GM) volumes, C2–C3 spinal cord area, and functional connectivity (FC) from nine resting-state networks (RSNs) were compared. Step-wise logistic regressions tested PIRMA predictors among clinical and structural MRI features, RSNs, and kernel principal component analysis (k-PCA) characteristics.

Results: Of 208 patients, 99 were excluded for clinical ($n=30$) and MRI activity ($n=69$). Among 109, 33% experienced PIRMA. PIRMA progressors were older, more disabled, had higher WM lesion volume, GM atrophy, and FC alterations. Logistic regressions identified higher EDSS ($p<0.001$), age ($p=0.02$), cortical atrophy ($p=0.04$), and FC alterations as predictors (all $p\leqslant 0.02$). Six k-PCA components emerged; four (linked to GM atrophy, FC decrements, age, EDSS) predicted PIRMA (pseudo-$R^2=0.61$).

Conclusion: PIRMA is linked to aging, GM atrophy, and disrupted FC, highlighting the value of integrating structural and functional MRI markers to detect silent progression in MS.

Keywords: Multiple sclerosis, functional MRI, PIRMA, silent progression, structural MRI

Date received: 13 December 2025; revised: 26 March 2026; accepted: 9 April 2026

Correspondence to:
E Barbuti
Department of Human Neurosciences, Sapienza University of Rome, Viale dell'Università 30, 00185, Rome, Italy.
elena.barbuti@uniroma1.it

Elena Barbuti
Claudia Piervincenzi
Viola Baione
Abhineet Ojha
Federica Satriano
Carlo Pozzilli
Department of Human Neurosciences, Sapienza University of Rome, Rome, Italy

Antonio Gallo
Alessandro D'Ambrosio
Department of Advanced Medical and Surgical Sciences and 3T MRI Center, University of Campania "Luigi Vanvitelli", Naples, Italy; First Division of Neurology and Neurophysiopathology, AOU Luigi Vanvitelli, Naples, Italy

Nicola De Stefano
Rosa Cortese
Department of Medicine, Surgery and Neuroscience, University of Siena, Siena, Italy

Paola Valsasina
Neuroimaging Research Unit, Division of Neuroscience, IRCCS San Raffaele Scientific Institute, Milan, Italy

Maria A Rocca
Neuroimaging Research Unit, Division of Neuroscience, IRCCS San Raffaele Scientific Institute, Milan, Italy; Neurology Unit, IRCCS San Raffaele Scientific Institute, Milan, Italy; Vita-Salute San Raffaele University, Milan, Italy

Massimo Filippi
Neuroimaging Research Unit, Division of Neuroscience, IRCCS San Raffaele Scientific Institute, Milan, Italy; Neurology Unit, IRCCS San

Introduction

Disability accrual in multiple sclerosis (MS) arises from two distinct but not mutually exclusive phenomena: relapse-associated worsening (RAW) and progression independent of relapse activity (PIRA).[1] RAW has been defined as a confirmed disability progression (CDP) event occurring within 90 days following a relapse or up to 30 days before it, while PIRA indicates CDP events outside this time window.[2] As the PIRA definition does not account for new asymptomatic magnetic resonance imaging (MRI) lesions, the term PIRMA (progression independent of relapse and MRI activity) was introduced.[3] Including new MRI lesions in the definition of PIRA has halved the number of events,[4] suggesting that asymptomatic central nervous system lesions may account for a significant portion of PIRA.[5] However, these definitions are limited by arbitrary time frames, as inflammation-related damage might persist beyond them: white matter (WM) lesions have been shown to predict abnormalities in normal appearing WM and gray matter (GM) up to 2 years,[6] and microstructural

Raffaele Scientific Institute, Milan, Italy; Vita-Salute San Raffaele University, Milan, Italy; Neurorehabilitation Unit, IRCCS San Raffaele Scientific Institute, Milan, Italy; Neurophysiology Service, IRCCS San Raffaele Scientific Institute, Milan, Italy

Patrizia Pantano
Department of Human Neurosciences, Sapienza University of Rome, Rome, Italy; IRCCS NEUROMED, Pozzilli, Italy

*INNI Network: Nikolaos Petsas (School of Medical Statistics and Biometry, Dept of Public Health and Infectious Diseases, Sapienza University of Rome), Silvia Tommasin (Department of Human Neurosciences, Sapienza University of Rome, Rome, Italy; UniCamillus-International Medical University in Rome, Rome, Italy), Loredana Storelli (Neuroimaging Research Unit, Division of Neuroscience, IRCCS San Raffaele Scientific Institute, Milan, Italy), Nicolò Tedone (Neuroimaging Research Unit, Division of Neuroscience, IRCCS San Raffaele Scientific Institute, Milan, Italy; Neurology Unit, IRCCS San Raffaele Scientific Institute, Milan, Italy), Stefania Sala (Neuroimaging Research Unit, Division of Neuroscience, IRCCS San Raffaele Scientific Institute, Milan, Italy), Elisabetta Pagani (Neuroimaging Research Unit, Division of Neuroscience, IRCCS San Raffaele Scientific Institute, Milan, Italy), Paolo Preziosa (Neuroimaging Research Unit, Division of Neuroscience, IRCCS San Raffaele Scientific Institute, Milan, Italy), Alvino Bisecco (Department of Advanced Medical and Surgical Sciences, and 3T MRI Center, University of Campania "Luigi Vanvitelli", Naples, Italy), Riccardo Borgo (Department of Advanced Medical and Surgical Sciences, and 3T MRI Center, University of Campania "Luigi Vanvitelli", Naples, Italy), Valentina Rippa (Department of Advanced Medical and Surgical Sciences, and 3T MRI Center, University of Campania "Luigi Vanvitelli", Naples, Italy), Fabrizio Esposito (Department of Advanced Medical and Surgical Sciences, and 3T MRI Center, University of Campania "Luigi Vanvitelli", Naples, Italy), Manuela

changes may precede visible lesions by months.[7] We defined PIRMA as a CDP event occurring without relapses or MRI activity throughout a 5-year follow-up period.

Previous studies evaluated MRI markers predictive of silent progression, with the caveat that definitions did not fully exclude the neuro-inflammatory component, and mainly focused on structural MRI features.[8,9] Functional connectivity (FC) disruption has been associated with EDSS progression, but its role in silent progression prediction has not yet been explored.[10,11] In this study, we investigated FC measures as predictors of PIRMA, integrating them with structural MRI and clinical variables in a multimodal predictive approach. Moreover, we assessed their prognostic value over a medium follow-up period of 5 years, to provide a comprehensive characterization of the mechanisms underlying silent disability progression in MS.

Materials and methods

Study design

MS patients were retrospectively retrieved from the Italian Neuroimaging Network Initiative (INNI) repository (https://database.inni-ms.org), which includes clinical and MRI data from four Italian MS Research Centers (IRCCS San Raffaele Scientific Institute, Milan; Sapienza University of Rome; University Campania "Luigi Vanvitelli," Naples; University of Siena).[12]

The study protocols were approved by the local ethics committees and performed in accordance with the ethical standards laid down in the 1964 Declaration of Helsinki. All patients signed a written informed consent form. All data were anonymized to protect the subjects' privacy. The inclusion criteria for the INNI database have been reported elsewhere.[12] Patients experiencing clinical relapses within 3 months or receiving corticosteroid treatment within 1 month before MRI were excluded.

We retrospectively identified patients with availability of demographics (age, sex), clinical data (disease duration, phenotype, treatment status, Expanded Disability Status Scale (EDSS)), and two MRI scans acquired with the same scanner, 4 to 6 years apart. We excluded patients who experienced clinical relapses or showed any MRI activity (new T2 or gadolinium-enhancing T1 lesions) at any point during the 5-year follow-up. Only patients without any clinical or radiological inflammatory activity during the observation period were included in the final cohort. Among them, we classified patients as PIRMA progressors or stable according to CDP. CDP was defined as a 3-month confirmed EDSS score increase of 1.5, 1.0, or 0.5 from a baseline score of 0, 1.0–5.5, and ⩾6, respectively.[13] We defined PIRMA as a CDP event occurring in the absence of relapses or MRI activity during the follow-up. Relapses were defined as the appearance of new/return of old neurological symptoms for at least 24 hours, without infection or body temperature change.

Treatment status was categorized as no treatment, low- to medium-efficacy (interferons, glatiramer acetate, dimethyl fumarate, and teriflunomide), and high-efficacy (S1P modulators, cladribine, monoclonal antibodies) disease-modifying treatments (DMTs). Non-MS-specific immunosuppressive treatments (methotrexate, mitoxantrone, azathioprine, cyclophosphamide) were considered separately.

MRI acquisition

MRI scans were obtained using 3.0T scanners. At baseline, from the MRI protocol, we selected three-dimensional (3D) T1-weighted, proton-density (PD)/T2-weighted, and/or Fluid-Attenuated Inversion Recovery (FLAIR) images, along with resting-state fMRI and, when available, post-contrast T1-weighted images. Acquisition details are provided in Supplemental Table 1. For our purposes, only PD/T2-weighted/FLAIR images and, when available, post-contrast T1-weighted images were retrieved from follow-up MRI.

MRI activity assessment

T2-weighted images were compared between baseline and follow-up MRI scans by visual inspection to identify new WM lesions by two neurologists with 4 years of experience in neuroimaging analysis (E.B. and V.B.). When available, post-contrast T1 images were also inspected to identify gadolinium-enhancing lesions.

Baseline MRI analysis

Pre-processing. Structural and functional images were pre- and post-processed using fMRIPrep v20.2.3[14] and the FMRIB Software Library (FSL, version 6.0.7.13) (https://fsl.fmrib.ox.ac.uk/fsl/fslwiki). Pipelines are described in the Supplemental Materials.

Structural MRI

WM lesion volume. T2-hyperintense WM lesions were segmented using a local thresholding segmentation technique (Jim 9.0, Xinapse System, Colchester, UK; http://www.xinapse.com), and WM lesion volumes were calculated with fslstats "FSL."

Global and regional brain volumes. 3D-T1 images were lesion-filled FMRIB Software Library tool (FSL, version 6.0.0). SIENAx2[15] was used to extract cortical, thalamic, striatal (sum of caudate and putamen nuclei), and WM volumes from lesion-filled T1 brain images. For each deep GM structure, the left and right volumes were summed. All volumes were normalized to the V scaling factor.

Spinal cord cross-sectional area. Spinal cord cross-sectional area (SCA) at C2–C3 was computed on bias-corrected 3D-T1 images from the brain using Spinal Cord Toolbox v 5.0.1 (SCT). Segmentation was performed with the *sct_propseg* algorithm, followed by vertebral labeling with *sct_label_vertebrae* aligned to the PAM50 template. Labeling accuracy was verified at the C2–C3 intervertebral disk. In case of automated labeling failure, manual labeling of the posterior tip of the intervertebral disk C2–C3 was carried out with *sct_label_utils*.

Functional MRI. Independent component analysis (ICA) was performed using MELODIC (FSL) at the group level by temporally concatenating preprocessed fMRI data into a single four-dimensional (4D) data set. Group ICA was set to 20 components.[16] Nine resting-state networks (RSNs) were selected based on spatial correlations (*fslcc* tool) with template RSNs from Smith et al.[16] and Yeo et al.[17] and confirmed by expert visual inspection: sensory-motor network (SMN), dorsal attention network (DAN), default-mode network (DMN), executive control network (ECN), right fronto-parietal network (FPR), left fronto-parietal network (FPL), occipital network (OCN), medial visual network (MVN), and cerebellar network (CBN).

The group-level spatial maps were used to derive subject-specific maps and time series through a dual regression approach.[18] The group spatial maps were regressed into each subject's 4D data set to obtain subject-specific time series, which were then regressed into the same data set, yielding individual spatial maps corresponding to each group-level component.

Feature harmonization. To account for scanner-related variability, we applied ComBat harmonization to all volumetric measures and separately to each RSN.[19] Age and sex were included as biological covariates.

Statistical analysis

R software v.4.3.3 and SPSS Statistics software v.28.0.1.1 were used. Normality in measurements was tested with the Kolmogorov–Smirnov test and visual inspection. Nonparametric/parametric tests were used according to whether the data were non-normally or normally distributed. Unpaired two-sample *t*-test, chi-square test, and Mann–Whitney U-test were used to assess differences in demographic variables and structural MRI features in patients undergoing PIRMA (PIRMA progressors) versus stable patients. Significance was stated if $p < 0.05$ after adjusting for multiple comparisons (Benjamini–Hochberg).

Subject-specific spatial maps obtained from dual regression analysis were entered into group-level voxel-wise analyses. For each RSN, FC differences between patients' groups were assessed using two-sample unpaired *t*-tests. Voxel-wise statistical analyses were performed with permutation-based non-parametric statistics using the FSL Randomise permutation-based program with 5000 permutations. Results were corrected using false discovery rate (FDR) correction for multiple comparisons ($p < 0.05$, cluster size larger than 100 voxels). Age, sex, WM lesion volume, and cortical volume were included as covariates of no interest. Anatomical localization of significant clusters was established according to the Harvard–Oxford cortical, subcortical, and cerebellar atlases included in the FMRIB's Software Library (http://www.fmrib.ox.ac.uk/fsl/data/atlasdescriptions.html).

Step-wise forward logistic regressions were fitted to test PIRMA predictors in separate models for (1) demographic/clinical features (age, sex, disease duration, phenotype, EDSS, treatment status); (2) structural MRI features (WM lesion, cortical, WM, thalamic, striatal volumes and SCA), adjusting for age and sex; (3) RSNs (mean value from the contrast maps obtained from the unpaired *t*-tests); and (4) components of all clinical, structural and functional MRI features, obtained through kernel principal component analysis (k-PCA) with a radial basis function (RBF) kernel, to reduce dimensionality.

k-PCA was chosen to capture potential non-linear relationships not adequately represented by linear approaches. Categorical variables were recorded as numeric factors. All variables were z-standardized

Altieri (Department of Advanced Medical and Surgical Sciences, and 3T MRI Center, University of Campania "Luigi Vanvitelli", Naples, Italy), Maria Laura Stromillo (Department of Medicine, Surgery and Neuroscience, University of Siena, Siena, Italy), Riccardo Tappa Brocci (Department of Medicine, Surgery and Neuroscience, University of Siena, Siena, Italy).

Data Availability Statement included at the end of the article.

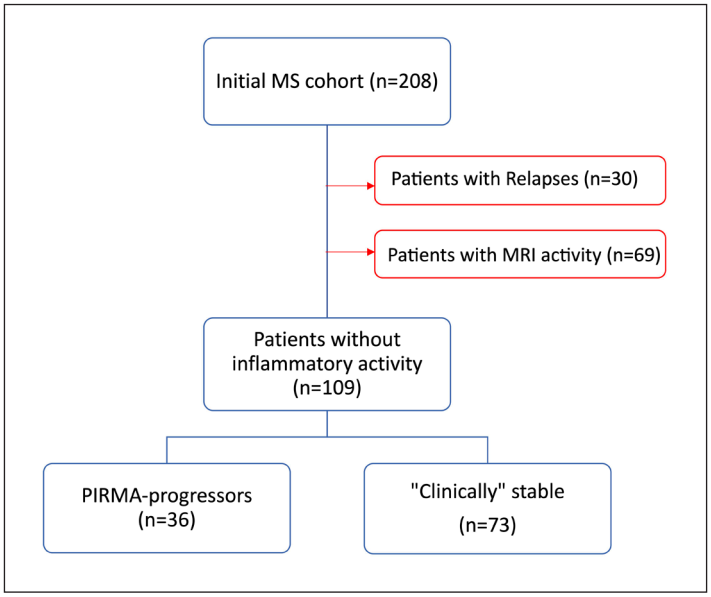

Figure 1. Study flowchart.

before dimensionality reduction. The first six non-linear components were retained, and correlations between the original variables and each component were calculated to aid interpretation. Multicollinearity among predictors was assessed using the variance inflation factor (VIF), with a cutoff of 5.

Results

Study population

From all records available in the INNI database, 208 MS patients were identified as having both clinical assessment and MRI data with the above-described protocol available at baseline and 5 years of follow-up. Post-contrast T1-weighted imaging, though not included in our protocol, was available in the original cohort at baseline for 98 patients and at follow-up for 57 patients, as performed for clinical practice. Thirty patients were excluded because of relapses and 69 because of MRI activity at follow-up (new T2 lesions, three of which showed gadolinium enhancement) (Figure 1). The final cohort comprised 109 patients without relapses or MRI activity during the 5-year follow-up: 79 (72.5%) females, mean age: 41 ± 9 years, mean disease duration: 11 ± 8 years, 92 relapsing and 17 progressive MS, with a median EDSS 2.0 (interquartile range (IQR): 2.5); 29 (26.6%) untreated, 57 (52.3%) on low- to medium-efficacy DMT (35 interferons, 11 glatiramer acetate, 8 dimethyl fumarate, and 3 teriflunomide), and 23 (21.1%) on high-efficacy DMT (17 fingolimod, 1 cladribine, and 5 natalizumab).

At 5-year follow-up, median EDSS was 2.5 (IQR 3), with a median baseline to follow-up EDSS change of 0 (IQR 1), 18 patients (16.5%) remained untreated, 54 (49.5%) were on low- to medium-efficacy DMT (26 interferons, 8 glatiramer acetate, 14 dimethyl fumarate, and 6 teriflunomide,), 33 (30.3%) on high-efficacy DMT (23 fingolimod, 1 ponesimod, 1 cladribine, and 8 natalizumab) and 4 (3.7%) had begun immunosuppressive drugs (two cyclophosphamide, one mitoxantrone, one methotrexate); 82 patients remained relapsing-remitting, while 10 converted to secondary-progressive MS (SPMS) (27 progressive MS patients at follow-up) according to Lorscheider et al. criteria.[20]

Demographic and clinical features

At 5-year follow-up, 36 of 109 patients (33%) developed PIRMA. Baseline demographic and clinical features of PIRMA progressors versus stable patients are shown in Table 1: progressors were older, had higher baseline EDSS, and longer disease duration ($p < 0.05$). No differences were found in treatment status at baseline, at follow-up ($p = 0.08$, $p = 0.11$), or in treatment changes during follow-up ($p = 0.18$).

Logistic regression (pseudo-R^2 (Nagelkerke) = 0.2) identified EDSS as the best PIRMA predictor (ß = 0.5, OR = 1.65, 95% CI = 1.28–2.14, $p < 0.001$).

Table 1. Demographic, clinical, and structural MRI characteristics of stable patients versus PIRMA progressors at baseline.

	Stable ($n=73$)	PIRMA progressors ($n=36$)	p (uncorrected)	FDR-p
Age, mean (SD), years	39.16 (8.83)	44.67 (9.2)	**0.003**[a]	**0.01**[a]
Female, *n* (%)	53 (72.6)	26 (72.2)	0.97[b]	0.97[b]
Disease duration, mean (SD), years	9.42 (7.84)	13.19 (7.24)	**0.009**[c]	**0.02**[c]
EDSS, median (range)	1.5 (0–6.5)	3.25 (1–6.5)	**<0.001**[c]	**<0.001**[c]
Phenotype, *n* (%)				
RMS	68 (93.15)	24 (66.67)	**0.001**[b]	**0.006**[b]
PMS	5 (6.85)	12 (33.33)		
Treatment at baseline (*n*, %)			0.08[b]	0.1[b]
No treatment	22 (30.14)	7 (19.44)		
Low–medium efficacy	40 (54.79) 28 interferons 7 glatiramer acetate 5 dimethyl fumarate	17 (47.22) 7 interferons 4 glatiramer acetate 3 dimethyl fumarate 3 teriflunomide		
High efficacy	11 (15.07) 1 cladribine 9 fingolimod 1 natalizumab	12 (33.34) 8 fingolimod 4 natalizumab		
WM lesion volume, mean (SD)	5658.29 (6412.59)	8896.7 (8752.47)	**0.03**[c]	**0.045**[c]
WM volume, mean (SD)	683.01 (51.39)	681.89 (64.73)	0.69[c]	0.75[c]
Cortical volume, mean (SD)	631.24 (42.48)	605.44 (57.15)	**0.009**[a]	**0.02**[a]
Thalamic volume, mean (SD)	21.22 (1.86)	20.17 (2.35)	**0.01**[a]	**0.02**[a]
Striatal volume, mean (SD)	22.9 (2.29)	21.59 (2.64)	**0.009**[a]	**0.02**[a]
Spinal cord area, mean (SD)	61.45 (9.83)	57.44 (9.5)	**0.05**[a]	0.07[a]

[a]*t*-Test for independent variables, equal variance tested with Levene.
[b]Chi-squared test.
[c]Mann–Whitney test.
Bold font indicates statistical significance.
All volumes are expressed in mm^3 and normalized for the V scaling factor (Siena X2), while spinal cord area is expressed as mm^2.

Structural MRI features

Progressors had greater WM lesion volume and cortical and subcortical GM atrophy ($p < 0.05$) (Table 1).

Logistic regression (pseudo-R^2 (Nagelkerke)$=0.2$) identified older age (ß$=0.06$, OR$=1.06$, 95% CI$=1.01$–1.12, $p=0.02$) and lower cortical volume (ß$=-0.01$, OR$=0.99$, 95% CI$=0.98$–0.99, $p=0.04$) as the best predictors of PIRMA.

Resting-state FC

Compared with stable patients, PIRMA progressors showed lower FC across several RSN, including MVN, DMN, ECN, FPR, OCN, and SMN (FDR corrected, $p < 0.05$) and higher FC in CBN and DAN (Figure 2 and Table 2). No differences in FC were found between the two groups in the FPL network.

Logistic regression (pseudo-$R^2=0.78$) identified FC abnormalities in SMN ($p=0.02$), DAN ($p=0.004$), DMN ($p=0.004$), FPR ($p=0.01$), OCN ($p=0.01$), and CBN ($p=0.002$) as predictors of PIRMA (Supplemental Table 2).

Combined demographic, clinical, structural, and functional MRI features

k-PCA was applied to six clinico-demographic, six structural, and eight functional MRI measures, identifying six non-linear components (Figure 3) that together explained 100% of the variance in the transformed feature space. The variance was evenly distributed (PC1: 26.65%, PC2: 19.12%, PC3: 15.55%, PC4: 14.04%, PC5: 12.94%, PC6: 11.7%), consistent with the absence of a single dominant axis and reflecting the complex structure of the data set. Correlations between variables and components are presented in Supplemental Table 3 with a cutoff > 0.3.

Step-wise logistic regression identified components from 1 to 4 as significant predictors of

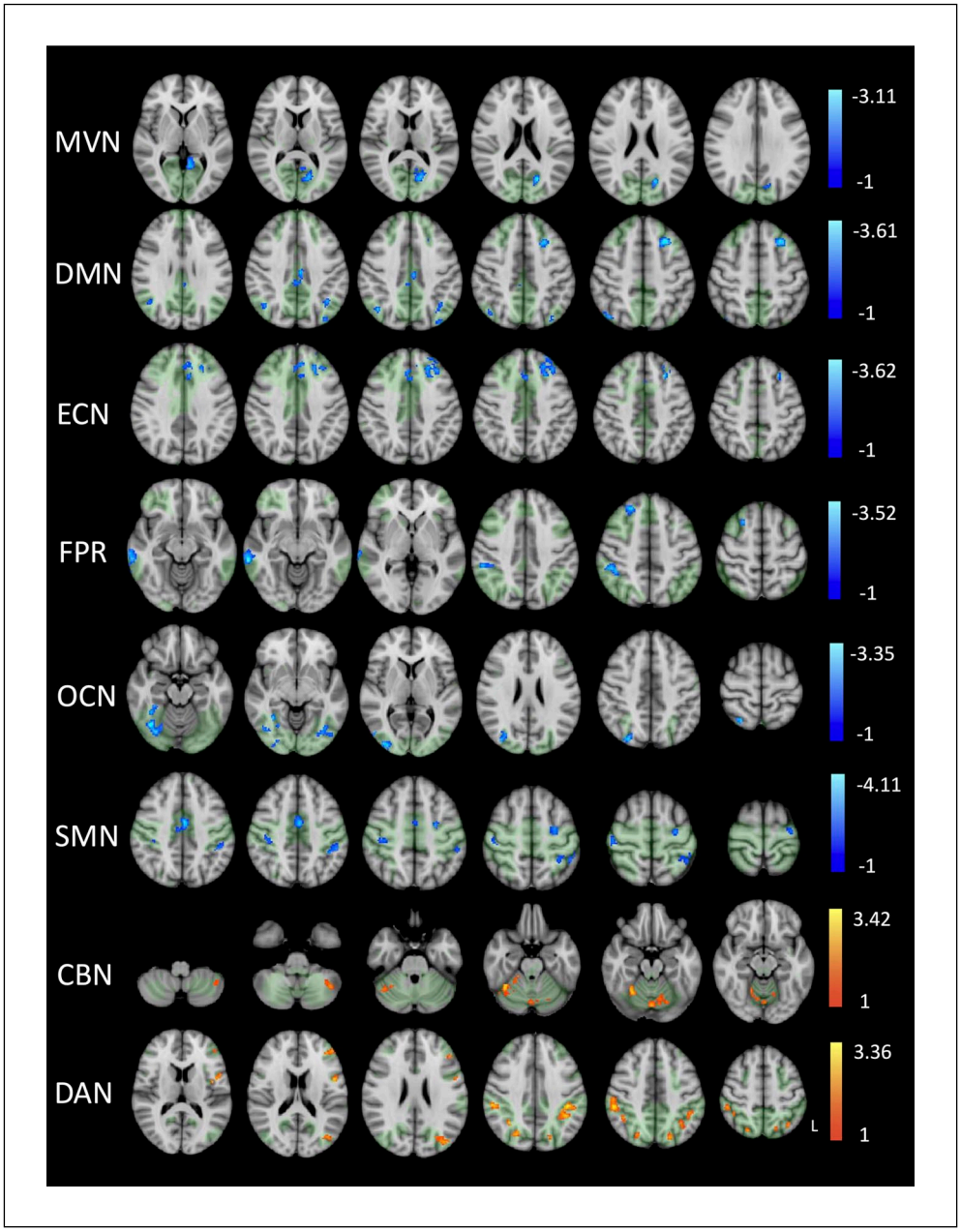

Figure 2. Resting-state networks (RSNs) showing significant functional connectivity (FC) differences between PIRMA progressors and stable patients ($p < 0.05$, FDR corrected). Results for each RSN are overlaid onto the corresponding network (green) in the MNI152 standard brain. Significant clusters of lower FC in PIRMA progressors relative to stable patients are shown in blue-light-blue, while significant clusters of higher FC in PIRMA progressors relative to stable patients are shown in red-yellow (color bars represent *t* values).
CBN, cerebellar network; DAN, dorsal attention network; DMN, default-mode network; ECN, executive control network; FPR, fronto-parietal right network; MVN, medial visual network; OCN, occipital network; SMN, sensory-motor network.

PIRMA (pseudo-$R^2 = 0.61$, PC1 $p < 0.001$, PC3 $p < 0.001$, PC4 $p = 0.005$, PC2 $p = 0.007$, Supplemental Table 4). PC1 was mainly associated with GM volumes (thalamic, striatal, cortical), PC2 and PC3 with FC networks showing lower FC in PIRMA progressors (DMN, SMN, MVN, ECN, OCN), and PC4 with treatment status, SCA, EDSS, and phenotype.

Table 2. Clusters of FC decreased or increased in PIRMA progressors relative to stable patients.

	RSN	*k* (voxels)	*t*	MNI coordinates (*x*, *y*, *z*)	Anatomical label
FC decreased in PIRMA progressors	MVN	459	3.11	−14, −70, 12	L. intracalcarine cortex
			3	−10, −54, 2	L. lingual gyrus
	DMN	152	3.61	−26, 20, 50	L. superior frontal gyrus
		142	3.5	−38, −56, 36	L. angular gyrus
			2.83	−34, −78, 34	L. lateral occipital cortex (superior division)
		131	3.06	42, −64, 40	R. lateral occipital cortex (superior division)
		115	3.12	−4, −20, 38	L. cingulate gyrus (posterior division)
			2.3	2, −34, 38	R. cingulate gyrus (posterior division)
	ECN	244	3.62	−24, 24, 46	L. superior frontal gyrus
			2.83	−26, 46, 42	L. frontal pole
			2.61	−34, 28, 42	L. middle frontal gyrus
		128	2.85	−10, 32, 36	L. paracingulate gyrus
			2.41	−6, 38, 38	L. superior frontal gyrus
	FPR	273	3.52	64, −34, −10	R. middle temporal gyrus (posterior division)
			2.23	62, −24, 4	R. superior temporal gyrus (posterior division)
			1.82	66, −44, −14	R. inferior temporal gyrus (temporooccipital part)
		176	3.08	46, −38, 48	R. supramarginal gyrus (posterior division)
		147	3.17	24, 34, 46	R. superior frontal gyrus
	OCN	339	3.35	38, −64, −16	R. occipital fusiform gyrus
			3.11	38, −46, −14	R. temporal occipital fusiform cortex
			2.83	34, −38, −18	R. temporal fusiform cortex(posterior division)
		288	3	28, −76, 46	R. lateral occipital cortex (superior division)
		214	3.02	34, −90, 6	R. occipital pole
			2.98	38, −88, 6	R. lateral occipital cortex (inferior division)
			2.23	26, −86, −10	R. occipital fusiform gyrus
			1.94	32, −94, −4	R. occipital pole
		122	2.98	44, −70, −2	R. lateral occipital cortex (inferior division)
		108	2.51	−46, −76, −12	L. lateral occipital cortex (inferior division)
			2.48	−40, −66, −10	L. occipital fusiform gyrus
	SMN	188	3.17	−44, −42, 44	L. supramarginal gyrus (posterior division)
			2.21	−30, −46, 54	L. superior parietal lobule
		171	4.11	−2, −6, 44	L. cingulate gyrus (anterior division)
			2.13	6, −16, 42	R. cingulate gyrus (posterior division)
		149	3.23	−24, −8, 52	L. precentral gyrus
		118	2.78	46, −24, 62	R. postcentral gyrus
FC increased in PIRMA progressors	CBN	232	3.11	0, −74, −20	Vermis VI
			2.66	18, −56, −14	R. cerebellar lobule VI
			2.55	−20, −70, −22	L. cerebellar lobule VI
		210	3.42	38, −50, −24	R. cerebellar lobule VI
			2.54	40, −58, −32	R. cerebellar crus I
			2.5	20, −38, −24	R. cerebellar lobule V
		110	2.81	−34, −54, −38	L. cerebellar crus I
			2.64	−40, −58, −44	L. cerebellar crus II
			2.27	−40, −52, −54	L. cerebellar lobule VIIb
	DAN	340	3.33	54, −34, 46	R. supramarginal gyrus (anterior division)
			2.95	34, −54, 38	R. angular gyrus
			2.52	42, −46, 50	R. superior parietal lobule
		282	3.36	−42, −34, 38	L. supramarginal gyrus (anterior division)
			2.89	−40, −46, 40	L. supramarginal gyrus (posterior division)
			2.46	−36, −62, 50	L. lateral occipital cortex (superior division)
			2.33	−32, −54, 44	L. superior parietal lobule
		209	3.09	−30, −66, 32	L. lateral occipital cortex (superior division)
		121	2.87	24, −70, 50	R. lateral occipital cortex (superior division)
		119	2.71	−48, 44, 16	L. frontal pole
			2.48	−44, 32, 24	L. middle frontal gyrus
		115	2.93	−50, 4, 18	L. precentral gyrus
			2.74	−42, −2, −12	L. central opercular cortex
		100	3.15	−20, −74, 42	L. lateral occipital cortex (superior division)

Clusters showing significant between-group differences in resting-state network connectivity. Cluster extent (k), *t*-values, peak MNI coordinates, and anatomical labels (based on the Harvard–Oxford atlas) are reported.

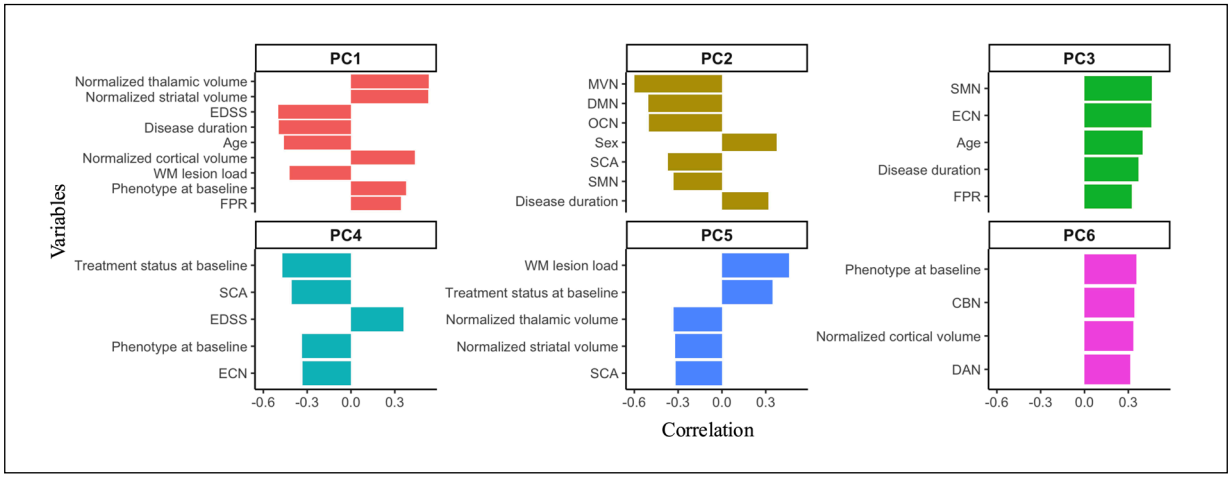

Figure 3. Correlations between original variables and the six components obtained with kernel principal component analysis (k-PCA).
CBN, cerebellar network; DAN, dorsal attention network; DMN, default-mode network; ECN, executive control network; EDSS, Expanded disability Status Scale; FPR, fronto-parietal right network; MVN, medial visual network; OCN, occipital network; SCA, spinal cord area; SMN, sensory-motor network; WM, white matter.

Discussion

Among MS patients without new MRI lesions or relapses over 5 years, 33% experienced PIRMA. Progressors were older, had longer disease duration and higher baseline disability, more pronounced GM atrophy, and widespread FC alterations in RSNs. By integrating FC measures with established clinical and structural MRI markers, our work provides a more comprehensive approach to detecting "silent" progression in MS.

Demographic/clinical risk factors for silent progression

Age was retained in our step-wise regression model and contributed to the most predictive components for PIRMA[1,3]. Older age has been consistently identified as the main predictor of PIRA, with a 1.6% increase in event rate per decade.[1,4,21] Mechanisms such as immunosenescence and inflammaging were shown to be responsible for Experimental Autoimmune Encephalomyelitis severity in aged mice.[22] However, in older individuals, EDSS may capture age-related disability rather than MS-specific impairment, as shown by a median score of 3 in non-MS subjects over 55 years.[23] PIRA/PIRMA definitions might be partially biased by the limited specificity of EDSS in older populations.

We found no significant predictive value for sex in our models, consistent with previous findings.[21] An Italian study found women had a higher PIRA/PIRMA risk, especially post-menopause, while men reached higher EDSS at follow-up.[24] MRI predictors were not analyzed.

In our cohort, disease duration and baseline EDSS were both associated with PIRMA-predictive components (1–3 and 1, 4, respectively), with EDSS showing the strongest predictive power among clinical variables in the step-wise regression model. These findings align with previous studies associating longer disease duration and higher baseline disability with increased PIRA risk.[1,2,4]

Phenotype at baseline did not emerge as a primary predictor of PIRMA despite a higher proportion of progressive patients among PIRMA progressors (Table 1). PIRA can occur in the early MS stages[4] and does not always result in SPMS conversion, especially if not sustained over time.[25] The coexistence of multiple disability trajectories within the same patient supports a unified view of MS beyond traditional phenotypes.[1]

Treatment at baseline showed only a partial relationship with PIRMA, correlating with the fourth (predictive) and fifth (non-predictive) components. We observed a trend toward a higher proportion of patients on high-efficacy therapies among PIRMA progressors (Table 1), likely reflecting a treatment selection bias, as patients with greater lesion burden and higher disability are typically prescribed more effective therapies. Moreover, a higher suppression of relapses and MRI activity could have unmasked silent progression, as already described.[3]

Structural MRI risk factors for silent progression

In our cohort, both cortical and deep GM volumes were associated with PIRMA progression, unlike

WM volume, in line with previous findings.[26] In a propensity score–matched analysis, patients with PIRA exhibited a lower parenchymal fraction and accelerated brain volume loss, mainly driven by cortical GM loss and cortical thinning, relative to stable patients.[8] A specific Cerebrospinal fluid (CSF) profile enriched in Tumor Necrosis Factor superfamily molecules related to meningeal and perivascular inflammation has been associated with PIRA/PIRMA, together with cortical lesion number, cortical thickness of the frontal cortex, and thalamic atrophy.[27] A CSF-mediated gradient of neuroaxonal loss and increased microglial density in the thalamus and cortex further supports a role for soluble inflammatory factors, related to meningeal and subependymal lymphoid-like infiltrates, in driving tissue damage and silent progression.[28]

WM lesion load was not a predominant feature in progression prediction. Lesion location in critical cross-signaling pathways and lesion heterogeneity, as captured by advanced MRI techniques such as susceptibility, quantitative, and diffusion imaging, could better reflect neuroaxonal damage and Wallerian degeneration contributing to disability accrual. Paramagnetic rim lesions and slowly expanding lesions have been associated with increased PIRA due to their size, tendency to enlarge, and greater tissue damage.[9,29] Similarly, microstructural damage in key WM tracts has been related to PIRA over a 4-year follow-up.[30]

In our cohort, SCA was only partially related to silent progression, being retained in the second and fourth but not the fifth component. Previous work related baseline spinal cord atrophy and accelerated atrophy rates to PIRA.[9]

Functional MRI risk factors for silent progression

In our study, FC was lower in PIRMA progressors compared with stable patients across some RSN (MVN, DMN, ECN, FPR, OCN, SMN) and was higher in PIRMA progressors compared with stable patients in CBN and DAN. RSN showing reduced connectivity were related to the components predicting PIRMA.

FC appears to increase early in MS as part of network reorganization and decrease with greater disease duration and aging.[31,32] A compensatory mechanism has been proposed in the early stages to counteract structural damage, leading to higher and widespread brain activation and inversely relating to disability.[33,34] Even though no previous work assessed FC alterations' role in predicting silent progression, several studies reported an association between network dysfunction and disability progression. In a 2-year longitudinal study with a graph theory approach, depletion of FC enhancement was significantly associated with disability progression, arguing for a progressive failing of compensatory mechanisms during the disease course.[11] However, another 5-year longitudinal study found no associations between connectome stability, proposed as an FC global measure, and physical or cognitive progression.[35] Differences in baseline disability could account for different trajectories of FC increase or decrease at follow-up, mainly due to patients' different locations in the curve of brain functional compensation in the theoretical model of network collapse.[11,32] A recent longitudinal study supported this theory, showing a disability-dependent evolution of FC: increased FC in low-disability patients correlated with better outcomes, while decreased FC in more disabled patients predicted worsening.[36] In our cohort, patients undergoing PIRMA were already at baseline older and more disabled, featuring a reduced FC in most of the networks explored. We did not find any specificity for a particular network in driving silent progression. Previous studies identified SMN and DMN as predictors of upper and lower limb disability[37] and EDSS progression.[10] In our study, PIRMA progressors were defined by EDSS, which explores several domains, probably lacking specificity toward a specific network dysfunction. Nevertheless, reduced FC in several RSNs was predictive of silent progression, meaning that the disruption of brain functional architecture could be an underlying mechanism of progression independent of acute inflammation.

Limitations

This study has some limitations. First, PIRMA was defined only by EDSS because of the lack of hand performance or speed walking measures, underestimating the assessment of silent progression. Furthermore, we were not able to evaluate the contribution of cortical lesions, paramagnetic rim lesions, or spinal cord lesions to PIRMA, because of the unavailability of standardized sequences and spinal cord MRIs in our multi-centric cohort. Moreover, post-gadolinium T1 sequences were not available for all cases, limiting the assessment of MRI activity to the presence of new T2 lesions at a follow-up MRI. Since gadolinium-enhancing lesions correspond to new or enlarging T2 lesions when compared with prior scans, and patients with clinical relapses were excluded, the only potential scenario in which MRI activity might

have been missed would be the presence of asymptomatic gadolinium enhancement in pre-existing lesions, which is relatively uncommon.

Conclusion

In our study, PIRMA was associated with a combination of predictors, including age, disability at baseline, GM atrophy, and disrupted FC, supporting the relevance of integrated structural and functional MRI markers for identifying silent disease progression. Understanding PIRMA-related mechanisms may enhance early identification of patients at risk for silent disability progression, supporting more personalized monitoring and the development of therapeutic strategies that target neurodegeneration and functional network disruption beyond inflammatory activity.

Declaration of Conflicting Interests

The authors declared the following potential conflicts of interest with respect to the research, authorship, and/or publication of this article: Elena Barbuti was awarded an ECTRIMS Clinical Fellowship 2025. Claudia Piervincenzi receives research support from the Fondazione Italiana Sclerosi Multipla. Viola Baione has nothing to disclose. Abhineet Ojha has nothing to disclose. Federica Satriano has nothing to disclose. Antonio Gallo has received speaker and consulting fees from Biogen, Genzyme, Merck Serono, Mylan, Novartis, Roche, and Teva and received research support from Fondazione Italiana Sclerosi Multipla. Alessandro d'Ambrosio has nothing to disclose. Manuela Altieri has nothing to disclose. Nicola De Stefano has received honoraria from Biogen Idec, Bristol Myers Squibb, Celgene, Genzyme, Immunic, Merck Serono, Novartis, Roche, and Teva for consulting services, speaking, and travel support. He serves on advisory boards for Merck, Novartis, Biogen Idec, Roche, and Genzyme, Immunic, and he has received research grant support from the Italian MS Society. Rosa Cortese was awarded a MAGNIMS-ECTRIMS fellowship in 2019; she received speaker honoraria from Roche, Merck Serono, and Sanofi and travel support for conferences by Novartis. Paola Valsasina has received speaker honoraria from Biogen Idec. Carlo Pozzilli has served on scientific advisory boards for Novartis, Merck, Biogen, Sanofi, Genzyme, Teva, and Actelion; received funding for travel and speaker honoraria from Biogen, Teva, Sanofi-Genzyme, Actelion, and Novartis; received research support from Biogen, Teva, Novartis, and Genzyme. Maria A. Rocca has received consulting fees from Biogen, Bristol Myers Squibb, Eli Lilly, Janssen, and Roche, and speaker honoraria from AstraZeneca, Biogen, Bristol Myers Squibb, Bromatech, Celgene, Genzyme, Horizon Therapeutics Italy, Merck Serono SpA, Novartis, Roche, Sanofi, and Teva. She receives research support from the MS Society of Canada, the Italian Ministry of Health, the Italian Ministry of University and Research, and Fondazione Italiana Sclerosi Multipla. She is Associate Editor for Multiple Sclerosis and Related Disorders. Massimo Filippi is Editor-in-Chief of the Journal of Neurology, Associate Editor of Human Brain Mapping, Neurological Sciences, and Radiology; received compensation for consulting services from Alexion, Almirall, Biogen, Merck, Novartis, Roche, and Sanofi; speaking activities from Bayer, Biogen, Celgene, Chiesi Italia SpA, Eli Lilly, Genzyme, Janssen, Merck Serono, Neopharmed Gentili, Novartis, Novo Nordisk, Roche, Sanofi, Takeda, and Teva; participation in Advisory Boards for Alexion, Biogen, Bristol Myers Squibb, Merck, Novartis, Roche, Sanofi, Sanofi-Aventis, Sanofi-Genzyme, and Takeda; scientific direction of educational events for Biogen, Merck, Roche, Celgene, Bristol Myers Squibb, Lilly, Novartis, and Sanofi-Genzyme; he receives research support from Biogen Idec, Merck Serono, Novartis, Roche, the Italian Ministry of Health, the Italian Ministry of University and Research, and Fondazione Italiana Sclerosi Multipla. Patrizia Pantano has received funding for travel from Novartis, Genzyme, and Bracco and speaker honoraria from Biogen. She receives research support from the Italian Ministry of Health, the Italian Ministry of University and Research, and Fondazione Italiana Sclerosi Multipla.

Funding

The authors disclosed receipt of the following financial support for the research, authorship, and/or publication of this article: This study was supported by FISM–Fondazione Italiana Sclerosi Multipla—cod. 2023/S/1 and financed or co-financed with the "5 per mille" public funding.

Ethics Consideration and Written Informed Consent

The study protocols were approved by the local ethics committees and performed in accordance with the 1964 Declaration of Helsinki. All patients signed a written informed consent form.

ORCID iDs

Elena Barbuti https://orcid.org/0000-0002-0450-7699
Claudia Piervincenzi https://orcid.org/0000-0002-7732-2062
Alessandro D'Ambrosio https://orcid.org/0000-0001-7729-4885
Nicola De Stefano https://orcid.org/0000-0003-4930-7639
Maria A Rocca https://orcid.org/0000-0003-2358-4320
Massimo Filippi https://orcid.org/0000-0002-5485-0479

Data Availability Statement

The data that support the findings of this study are available on request from the corresponding author. The data are not publicly available due to privacy or ethical restrictions.

Supplemental Material

Supplemental material for this article is available online.

References

1. Lublin FD, Häring DA, Ganjgahi H, et al. How patients with multiple sclerosis acquire disability. *Brain* 2022; 145: 3147–3161.
2. Kappos L, Wolinsky JS, Giovannoni G, et al. Contribution of relapse-independent progression vs relapse-associated worsening to overall confirmed disability accumulation in typical relapsing multiple sclerosis in a pooled analysis of 2 randomized clinical trials. *JAMA Neurol* 2020; 77: 1132.
3. Ciccarelli O, Barkhof F, Calabrese M, et al. Using the progression independent of relapse activity framework to unveil the pathobiological foundations of multiple sclerosis. *Neurology* 2024; 103: e209444.
4. Portaccio E, Bellinvia A, Fonderico M, et al. Progression is independent of relapse activity in early multiple sclerosis: A real-life cohort study. *Brain* 2022; 145: 2796–2805.
5. Maarouf A, Stellmann JP, Rico A, et al. Active and non-active progression independent of relapse activity within the first 20 years of relapsing multiple sclerosis. *J Neurol Neurosurg Psychiatry* 2024; 95: 974–978.
6. Bodini B, Chard D, Altmann DR, et al. White and gray matter damage in primary progressive MS: The chicken or the egg? *Neurology* 2016; 86: 170–176.
7. Filippi M, Rocca MA, Martino G, et al. Magnetization transfer changes in the normal appearing white matter precede the appearance of enhancing lesions in patients with multiple sclerosis. *Ann Neurol* 1998; 43: 809–814.
8. Cagol A, Schaedelin S, Barakovic M, et al. Association of brain atrophy with disease progression independent of relapse activity in patients with relapsing multiple sclerosis. *JAMA Neurol* 2022; 79: 682.
9. Cagol A, Benkert P, Melie-Garcia L, et al. Association of spinal cord atrophy and brain paramagnetic rim lesions with progression independent of relapse activity in people with MS. *Neurology* 2024; 102: e207768.
10. Rocca MA, Valsasina P, Meani A, et al. Network damage predicts clinical worsening in multiple sclerosis: A 6.4-year study. *Neurol Neuroimmunol Neuroinflamm* 2021; 8: e1006.
11. Faivre A, Robinet E, Guye M, et al. Depletion of brain functional connectivity enhancement leads to disability progression in multiple sclerosis: A longitudinal resting-state fMRI study. *Mult Scler* 2016; 22: 1695–1708.
12. Filippi M, Tedeschi G, Pantano P, et al. The Italian Neuroimaging Network Initiative (INNI): Enabling the use of advanced MRI techniques in patients with MS. *Neurol Sci* 2017; 38: 1029–1038.
13. Río J, Nos C, Tintoré M, et al. Defining the response to interferon-beta in relapsing-remitting multiple sclerosis patients. *Ann Neurol* 2006; 59: 344–352.
14. Esteban O, Markiewicz CJ, Blair RW, et al. fMRIPrep: A robust preprocessing pipeline for functional MRI. *Nat Methods* 2019; 16: 111–116.
15. Battaglini M, Jenkinson M, De Stefano N, et al. SIENA-XL for improving the assessment of gray and white matter volume changes on brain MRI. *Hum Brain Mapp* 2018; 39: 1063–1077.
16. Smith SM, Fox PT, Miller KL, et al. Correspondence of the brain's functional architecture during activation and rest. *Proc Natl Acad Sci USA* 2009; 106: 13040–13045.
17. Yeo BTT, Krienen FM, Sepulcre J, et al. The organization of the human cerebral cortex estimated by intrinsic functional connectivity. *J Neurophysiol* 2011; 106: 1125–1165.
18. Nickerson LD, Smith SM, Öngür D, et al. Using dual regression to investigate network shape and amplitude in functional connectivity analyses. *Front Neurosci* 2017; 11: 115.
19. Fortin J-P, Cullen N, Sheline YI, et al. Harmonization of cortical thickness measurements across scanners and sites. *NeuroImage* 2018; 167: 104–120.
20. Lorscheider J, Buzzard K, Jokubaitis V, et al. Defining secondary progressive multiple sclerosis. *Brain* 2016; 139: 2395–2405.

21. Prosperini L, Ruggieri S, Haggiag S, et al. Disability patterns in multiple sclerosis: A meta-analysis on RAW and PIRA in the real-world context. *Mult Scler* 2024; 30: 1309–1321.

22. Dema M, Eixarch H, Hervera A, et al. Disease aggravation with age in an experimental model of multiple sclerosis: Role of immunosenescence. *Aging Cell* 2025; 24: e14491.

23. Lynch S, Baker S, Nashatizadeh M, et al. Disability measurement in Multiple Sclerosis patients 55 years and older: What is the Expanded Disability Status Scale really telling clinicians? *Mult Scler Relat Disord* 2021; 49: 102724.

24. Foschi M, Marastoni D, Panzera I, et al. Sex differences in relapse-independent and relapse-associated disability progression in relapsing-remitting multiple sclerosis: A real-world inverse-probability weighted study. *Ther Adv Neurol Disord* 2025; 18: 17562864251376807.

25. Portaccio E, Betti M, De Meo E, et al. Progression independent of relapse activity in relapsing multiple sclerosis: Impact and relationship with secondary progression. *J Neurol* 2024; 271: 5074–5082.

26. Jacobsen C, Hagemeier J, Myhr K-M, et al. Brain atrophy and disability progression in multiple sclerosis patients: A 10-year follow-up study. *J Neurol Neurosurg Psychiatry* 2014; 85: 1109–1115.

27. Marastoni D, Colato E, Foschi M, et al. Intrathecal inflammatory profile and gray matter damage predict progression independent of relapse activity in early multiple sclerosis. *Neurol Neuroimmunol Neuroinflamm* 2025; 12: e200399.

28. Pardini M, Brown JWL, Magliozzi R, et al. Surface-in pathology in multiple sclerosis: A new view on pathogenesis? *Brain* 2021; 144: 1646–1654.

29. Calvi A, Vivó Pascual F, Solana E, et al. Diffusivity anisotropy signature of the slowly expanding lesions predicts progression independent of relapse activity in multiple sclerosis. *J Neurol Neurosurg Psychiatry* 2026; 97: 405–412.

30. Ocampo-Pineda M, Cagol A, Benkert P, et al. White matter tract degeneration in multiple sclerosis patients with progression independent of relapse activity. *Neurol Neuroimmunol Neuroinflamm* 2025; 12: e200388.

31. Tommasin S, De Giglio L, Ruggieri S, et al. Relation between functional connectivity and disability in multiple sclerosis: A non-linear model. *J Neurol* 2018; 265: 2881–2892.

32. Schoonheim MM, Meijer KA and Geurts JJG. Network collapse and cognitive impairment in multiple sclerosis. *Front Neurol* 2015; 6: 82.

33. Tommasin S, De Giglio L, Ruggieri S, et al. Multi-scale resting state functional reorganization in response to multiple sclerosis damage. *Neuroradiology* 2020; 62: 693–704.

34. Rocca MA, Schoonheim MM, Valsasina P, et al. Task- and resting-state fMRI studies in multiple sclerosis: From regions to systems and time-varying analysis. Current status and future perspective. *Neuroimage Clin* 2022; 35: 103076.

35. Høgestøl EA, Ghezzo S, Nygaard GO, et al. Functional connectivity in multiple sclerosis modelled as connectome stability: A 5-year follow-up study. *Mult Scler* 2022; 28: 532–540.

36. Piervincenzi C, Ojha A, Tommasin S, et al. Functional connectivity changes are associated with disability progression in multiple sclerosis: A longitudinal fMRI study. *J Neurol* 2025; 272: 787.

37. Strik M, Eijlers AJ, Dekker I, et al. Sensorimotor network dynamics predict decline in upper and lower limb function in people with multiple sclerosis. *Mult Scler* 2023; 29: 81–91.